Resonant inelastic light scattering in remotely doped wide parabolic GaAs/$Al_xGa_{1-x}As$ quantum wells

J. H. Burnett, H. M. Cheong, R. M. Westervelt, and W. Paul
Department of Physics and Division of Applied Sciences, Harvard University, Cambridge, Massachusetts 02138

P. F. Hopkins, M. Sundaram, and A. C. Gossard
Materials Department and Department of Electrical and Computer Engineering, University of California, Santa Barbara, Santa Barbara, California 93106

(Received 5 April 1993)

We have used resonant inelastic light-scattering spectroscopy in the depolarized backscattering configuration $z(y',x')\bar{z}$ to probe the single-particle excitations of two n-type remotely doped wide parabolic GaAs/$Al_xGa_{1-x}As$ quantum wells, with design curvatures corresponding to *empty* conduction-band harmonic-oscillator spacings of 4.4 and 3.3 meV. For the former sample, a series of spectra, for excitations near the $E_0+\Delta_0$ gap of the bulk material at the center of the well, reveal two light-scattering peaks with shifts ~ 0.85 and ~ 3.0 meV, which are strongly resonant with resonance widths of $\lesssim 3$ meV. Separate resonance curves were extracted, and the two resonance peaks are found to be separated by an energy approximately equal to the scattering peak separation. For the latter sample, similar spectra were obtained which reveal two strongly resonant light-scattering peaks with energy shifts ~ 0.65 and ~ 2.0 meV, with resonance maxima separated by an energy approximately equal to the scattering peak separation. We have interpreted these results in terms of single-particle transitions between conduction-band subbands and have found them quantitatively consistent with a model for the electron gas in the well distributed as a uniform density slab, giving rise to a square-well-like effective potential, as predicted for this system.

I. INTRODUCTION

Inelastic light scattering has been shown to be a useful technique for measuring electronic intersubband spacings in two-dimensional electron gas (2DEG) systems.[1,2] Following the proposal by Burstein, Pinczuk, and Buchner[3] to measure excitations in 2DEG's using inelastic light scattering and the observation by Pinczuk *et al.*[4] that both single particle and collective excitations in bulk n-type GaAs are strongly resonant near the $E_0+\Delta_0$ gap, Abstreiter and Ploog[1] reported evidence for intersubband transitions by carriers in the accumulation layer at a single GaAs/n-$Al_xGa_{1-x}As$ interface using this technique. Subsequently, Pinczuk *et al.*[2] reported observation by resonant inelastic light scattering of intersubband excitations of the multilayer 2DEG in modulation-doped GaAs/$Al_xGa_{1-x}As$ heterojunction superlattices. The intersubband energies measured were in good agreement with the calculated values for this structure.

This technique has been applied to other structures. Menéndez *et al.*[5] reported resonant inelastic light scattering in photoexcited parabolic GaAs/$Al_xGa_{1-x}As$ quantum wells (PBW's) to accurately measure the conduction-band harmonic-oscillator levels, with spacing ~ 25 meV. From these measurements they determined small deviations from parabolicity, and obtained the conduction-band offset. In this paper we report resonant inelastic light scattering in n-type remotely doped wide parabolic GaAs/$Al_xGa_{1-x}As$ quantum wells, a structure with altogether different characteristics from the empty PBW's investigated by Menéndez *et al.*[5]

Remotely doped wide parabolic GaAs/$Al_xGa_{1-x}As$ quantum wells have generated interest because they have been demonstrated to create relatively thick (>1000 Å) layers of uniform density, high-mobility electron gas,[6-9] and the properties of this electron gas are a subject of active research. As illustrated in Fig. 1(a), PBW's are created in the conduction band Γ_6 (CB), heavy- and light-hole valence bands Γ_8 (VB's), and spin-orbit split-off band Γ_7 (SOB) by varying the average Al concentration in a parabolic profile. For an empty PBW this results ideally in simple-harmonic-oscillator (SHO) energy levels for electrons, heavy holes, light holes, and spin-orbit split-off holes, with energy-level spacings given by $\hbar\omega_e^0$, $\hbar\omega_{hh}^0$, $\hbar\omega_{lh}^0$, and $\hbar\omega_{so}^0$, respectively, where for electrons $\omega_e^0=(K_{CB}/m_e^*)^{1/2}$. m_e^* is the electron effective mass and K_{CB} is the CB edge curvature given by $K_{CB}=d^2E_{CB}/dz^2=8\Delta E_{CB}/L_z^2$, where ΔE_{CB} is the difference between the energies at the center of the PBW and at the edge, and L_z is the width of the well. Analogous definitions apply for the hole levels.[10]

When electrons are added to the well by remote doping, for filling beyond single subband occupancy, self-consistent quantum-mechanical calculations[11] verify semiclassical arguments, that they become distributed as a slab with roughly uniform three-dimensional (3D) number density, $n^{3D}=2\Delta E_{CB}\varepsilon/\pi e^2L_z^2$. (Here, e is the electron charge and ε is the static dielectric constant.) The potential of this charged slab cancels the parabolic band-edge potential over the slab width w_e, which is propor-

tional to the filling, i.e., the sheet density n_s ($=w_e n^{3D}$). This leaves a flat-bottomed self-consistent potential in the CB over a width $\sim w_e$ and PBW's with greater curvatures $K_{CB}+K_{VB}$ and $K_{CB}+K_{SOB}$ in the VB's and the SOB, respectively, as indicated in Fig. 1(b), where K_{CB}, K_{VB}, and K_{SOB} are the curvatures for the corresponding empty PBW's. Furthermore, the 3D density and Fermi level are roughly independent of n_s, depending only on the bare parabolic curvature, and the occupied subband energy levels behave like a square-well spectrum $E_{n_e} \propto n_e^2/w_{\text{eff}}^2$. Here, n_e is the quantum number, and w_{eff} is an effective well width given by w_e plus a constant needed to account for the exponential tail of the wave function.[11] These predictions have been given support by transport measurements.[7,8] In this work we investigated the predicted square-well-like subband spacing in the CB with inelastic light scattering, using the harmonic-oscillator-like subbands in the SOB as resonance levels.

II. EXPERIMENT

The PBW samples were fabricated by molecule-beam epitaxy on (100) GaAs substrates, as described by Sundaram *et al.*[6] The parabolic band-edge variations were constructed from a 20-Å period superlattice, each period containing a GaAs and an $Al_xGa_{1-x}As$ layer, with the relative width of the two layers varied using a computer-controlled shutter to produce an average Al concentration with a parabolic profile, with x near zero at the center. The electrons were introduced into the CB well from Si-doped layers, set back symmetrically from both sides of the well with spacer layers in the $Al_xGa_{1-x}As$ barriers. We have made measurements on four PBW samples which showed similar effects. We will here discuss measurements on two samples. Sample 1 was grown with a nominal PBW width of $L_z=2800$ Å, with $x=0.005$ at the center and $x=0.2$ at the edge, giving a design density of $n^{3D}=1.22\times10^{16}$ cm^{-3}. It was symmetrically δ doped with spacer layers of 300 Å. The Hall-effect sheet density and mobility measured in the dark were $n_s=(1.7\pm0.2)\times10^{11}$ cm^{-2} and $\mu=0.8\times10^5$ cm^{2}V^{-1}sec^{-1}, respectively. The sheet density increased reversibly when exposed to light at low temperature. When illuminated at 2 K it saturated at $n_s=(1.8\pm0.2)\times10^{11}$ cm^{-2}, corresponding to a fractional filling of 0.53 and an effective well width of $w_{\text{eff}}=\sim1900\pm250$ Å. The Fermi level E_F determined by n^{3D} was 2.9 meV.

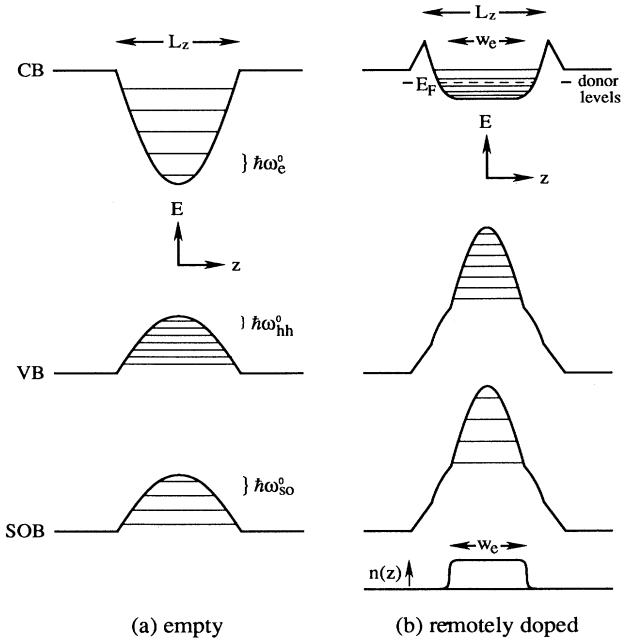

FIG. 1. Schematic diagram of the conduction-band edge, valence-band edge, and spin-orbit split-off band-edge profiles in (a) an empty $Al_xGa_{1-x}As$ parabolic well, with $k_x=k_y=0$ energy levels being simple-harmonic-like, and (b) an n-type remotely doped $Al_xGa_{1-x}As$ parabolic well, with $k_x=k_y=0$ energy levels being simple-harmonic-like in the VB and SOB, but square-well-like in the CB. (Only the heavy-hole levels in the VB are shown.) The effective width of the square well is given approximately by the width w_e of the electron slab indicated by the charge-density profile shown at the bottom of (b).

Sample 2 was grown with a nominal PBW width of $L_z=4640$ Å, with $x=0$ at the center and $x=0.3$ at the edge, giving a design density of $n^{3D}=6.8\times10^{15}$ cm^{-3}. It was symmetrically δ doped with spacer layers of 400 Å. The sheet density and mobility measured in the dark were $n_s=(1.4\pm0.2)\times10^{11}$ cm^{-2} and $\mu=2.4\times10^5$ cm^{2}V^{-1}sec^{-1}, respectively, and Shubnikov–de Haas measurements showed that three subbands were occupied. When exposed to light at 2 K the sheet density increased to $n_s=(1.7\pm0.2)\times10^{11}$ cm^{-2}, corresponding to a fractional filling of the well of 0.54 and an effective well width of $w_{\text{eff}}=\sim2900\pm400$ Å. The Fermi level E_F determined by n^{3D} was 1.9 meV.

The samples were cooled to 2 K using a He vapor flow optical cryostat, and excited with a dye laser, pumped by an Ar-ion laser. The inelastic light-scattering spectra were obtained using a double monochromator, with a cooled GaAs photomultiplier tube, photon counting electronics, and a computer-controlled data-acquisition system. The spectra were obtained in the depolarized backscattering configuration $z(y',x')\bar{z}$, with the incident photon energy $\hbar\omega_I$ (1.89–1.94 eV) near the $E_0+\Delta_0$ gap of GaAs. In this configuration the spectra are expected to exhibit electronic single-particle intersubband transitions.[12]

Recently it was shown by Pinczuk *et al.*[13] that with the depolarized configuration the dominant peaks actually correspond to spin-density excitations, which are shifted from the single-particle transition energies by the exchange Coulomb interaction. We assume, as is done in the other references cited here,[1–5,12,14–16] that this difference is small compared to the peak energy shift and width. This is especially justified here due to the low 3D densities of electron gases investigated. Thus we interpret the peaks as giving the energy spacing of the quantum well subbands.

III. MEASUREMENTS

Figure 2 shows a series of light-scattering spectra of sample 1, taken at 2 K, for excitation energies ranging

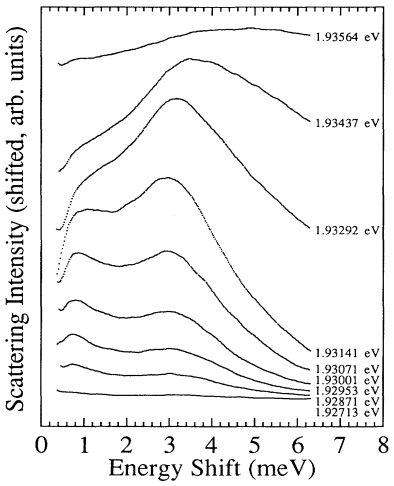

FIG. 2. Light-scattering spectra of sample 1 for various excitation energies shown to the right, taken in the $z(y',x')\bar{z}$ configuration at 2 K. Instrumental resolution is 0.1 meV. All spectra have the same scale factor and the top four are displaced vertically. The figure shows a peak at an energy shift of ~ 3.0 meV, resonant near 1.932 eV, and a peak at an energy shift of ~ 0.85 meV, resonant near 1.930 eV. The broad peak evident in the top two spectra is due to luminescence across the $E_0+\Delta_0$ gap.

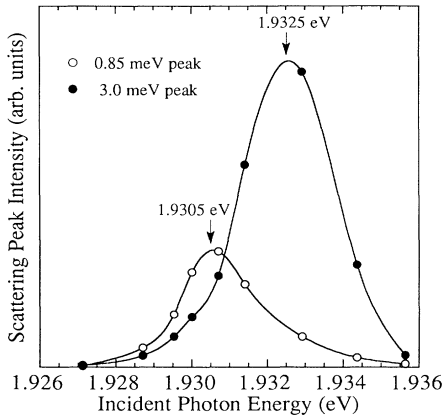

FIG. 3. Normalized scattering intensity for the peak maxima of the two light-scattering peaks of sample 1, as a function of incident photon energy. The solid lines are cubic spline fits to the data.

from 1.927 to 1.936 eV. The focused illumination power density was 5 W/cm^2 and the instrumental resolution was 0.1 meV. The spectra clearly show two peaks resonant at different excitation energies. Deconvolutions of the double peak structure with Lorentzians show that one peak has an energy shift of 3.0 ± 0.3 meV with a full width at half maximum (FWHM) of 3.2 ± 0.4 meV, which is resonant for excitations near 1.932 eV. The other peak has an energy shift of 0.85 ± 0.20 meV with a FWHM of 1.0 ± 0.2 meV, which is resonant for excitations near 1.930 eV. The two peaks are spaced apart by an energy of 2.15 ± 0.4 meV. (The upper three curves are seen to be distorted by a broad peak which has an increasing energy shift with increasing excitation energy. In fact, it has a constant peak energy, and is due to the weak luminescence across the $E_0+\Delta_0$ gap.) Resonant enhancement curves, showing the excitation energy dependence of the intensities of the two peaks at their maxima, determined from the deconvolution of the double peak structure for the various spectra, are shown in Fig. 3. These curves show a resonance width (FWHM) for the lowest energy shift peak of ~ 2.5 meV, and for the higher-energy shift peak of 3.0 meV. The resonant maxima for the two peaks differ by 2.0 ± 0.4 meV, approximately equal to the spacing between the two scattering peaks.

A series of light-scattering spectra with different excitation energies for sample 2, taken at 2 K, shows behavior similar to that observed for sample 1. The spectra reveal a peak with an energy shift of 2.0 ± 0.2 meV, which has maximum intensity for excitations near ~ 1.902 eV, and a much smaller peak with an energy shift of 0.65 ± 0.10 meV. The maximum intensities for the two peaks occur for excitations separated by an energy 1.5 ± 0.5 meV, approximately equal to the spacing between the two peaks.

Similar sets of measurements were made on these samples for different angles (from 0° to 45°) between the incident photon direction and the normal to the plane of the sample. For both samples the peak shifts were independent of this angle, eliminating the possibility of the peaks being associated with plasma oscillations.[12] The peak shifts were also independent of power for power densities ranging from 0.03 to 10 W/cm^2.

IV. DISCUSSION

The $z(y',x')\bar{z}$ light-scattering spectra of sample 1, shown in Fig. 2, display several noteworthy characteristics: (1) the spectra show peaks with energy shifts near 0.85 and 3.0 meV, which are strongly resonant with excitation energy resonance widths (FWHM) of $\lesssim 3$ meV, (2) the difference in energy between the shifts is approximately equal to the energy difference between the peaks of their respective resonance curves, and (3) the widths of the resonance curves are $\sim E_F \approx 2.9$ meV. These characteristics suggest a model similar to that proposed by Burstein, Pinczuk, and Buchner[3] and used by Pinczuk *et al.*[2] to analyze the inelastic $z(y',x')\bar{z}$ light-scattering spectra of modulation-doped GaAs/$Al_xGa_{1-x}As$ heterojunction superlattices, for which several peaks with energy shifts $\gtrsim 20$ meV and resonance widths $\gtrsim 30$ meV were observed. However, there are expected to be significant differences for the two cases. For the heterojunction superlattices studied by Pinczuk *et al.*,[2] the CB levels were relatively widely spaced ($\gtrsim 20$ meV) due to the narrow accumulation layerlike effective potentials in the CB, while the SOB levels were relatively narrowly spaced. For the case of remotely doped wide PBW's, however, the situation is reversed. The CB levels are expected to be relatively closely spaced (< 1 meV for the first few levels) due to the wide square-well-like effective potentials in the CB, but the SOB levels are expected to be more widely spaced (> 2.5 meV) due to the narrower PBW effective potentials.

In the scattering mechanism proposed by Burstein, Pinczuk, and Buchner[3] for the depolarized backscattering geometry $z(y',x')\bar{z}$, the peaks in the inelastic light-scattering spectra correspond to single-particle transitions from occupied CB subband states below the Fermi level to unoccupied CB subband states above the Fermi level, with opposite spin. These transitions can occur if the occupied intermediate states have mixed spins, due, for example, to the spin-orbit interaction, as in the SOB states. For incident and scattered photon wave vectors perpendicular to the heterostructure plane, the transitions must be vertical, i.e., the initial, intermediate, and final states must have the same value for the in-plane wave vector $\mathbf{k}$. Two such transitions for the remotely doped PBW structure are illustrated in the E versus $\mathbf{k}$ diagram in Fig. 4. Here, the initial and final states are in the square-well-level-like subbands of the CB and the intermediate states are in the harmonic-oscillator-level-like subbands of the SOB.

The matrix elements for these spin-flip intersubband transitions can be obtained from an extension to the case of a 2DEG of the matrix elements for a 3DEG, obtained by Wolff[14] and Hamilton and McWhorter.[15] For the case depicted in Fig. 4, where the intermediate state is a SOB subband state, the matrix element is given by[12,16]

$$M_{if}(\mathbf{k}) \propto |\hat{\mathbf{e}}_I \times \hat{\mathbf{e}}_S||P_{\mathrm{CB,SOB}}|^2 \sum_{\nu} \frac{\langle \phi_f(z)|e^{ik_I z}|\phi_\nu(z)\rangle\langle \phi_\nu(z)|e^{-ik_S z}|\phi_i(z)\rangle}{E(k,\nu)-\hbar\omega_I} . \tag{1}$$

Here, $\hat{\mathbf{e}}_I$, k_I, and ω_I are the unit polarization vector, wave vector, and frequency of the incident photons; $\hat{\mathbf{e}}_S$ and k_S are the corresponding quantities for the scattered photons; $\phi_i(z)$ and $\phi_f(z)$ are the square-well-like envelope functions of the initial- and final-state CB subbands; $\phi_\nu(z)$ are the harmonic-oscillator-like envelope functions of the intermediate-state SOB subbands; $\mathbf{k}$ is the two-dimensional in-plane wave vector common to all three states; $P_{\mathrm{CB,SOB}}$ is the momentum matrix element between the cell periodic parts of the CB and SOB wave functions; and $E(k,\nu)$ is the resonant energy given by

$$E(k,\nu)=E_G+E_f+E_\nu+\hbar^2k^2/2m_e^*+\hbar^2k^2/2m_{\mathrm{so}}^* , \tag{2}$$

where E_G is the $E_0+\Delta_0$ gap of bulk $Al_xGa_{1-x}As$ at the PBW minimum, E_f and E_ν are the $\mathbf{k}=0$ energies of the final- and intermediate-state subbands measured from the CB and SOB edges of bulk $Al_xGa_{1-x}As$ at the PBW minimum, and m_e^* and m_{so}^* are the effective masses of the CB and SOB subbands. The sum over ν in Eq. (1) is over all intermediate-state subbands. The total scattering intensity resulting from the transitions $i\rightarrow f$ is proportional to $|M_{if}(\mathbf{k})|^2$ summed over all $\mathbf{k}$ which correspond to an occupied initial CB subband state and an unoccupied final CB subband state.

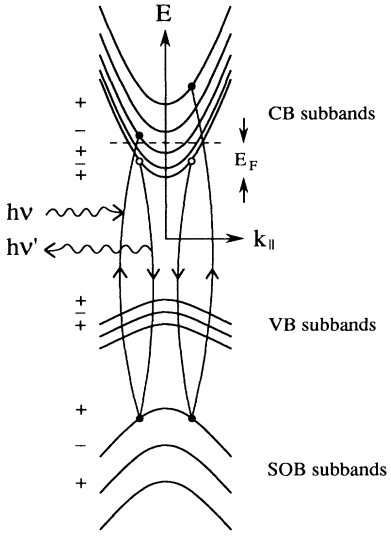

FIG. 4. Schematic diagram of several CB, VB, and SOB subbands for the remotely doped parabolic well shown in Fig. 1(b). Also shown are two vertical allowed inelastic scattering transitions, using a SOB subband state as intermediate state. The + and − signs on the left of the bands indicate the parity of the states.

The electric dipole approximation, $e^{ik_I z}\sim e^{-ik_S z}\rightarrow 1$, can be applied since $k_I\sim k_S \ll 1/L_{\mathrm{WF}}$, where L_{WF} is the size of the wave function of the smallest extent in Eq. (1), namely $\phi_\nu(z)$ with $L_{\mathrm{WF}}\sim 400$ Å for $\nu=1$. In this case, the selection rules are determined by the product of the envelope function overlap integrals,

$$\langle \phi_f(z)|\phi_\nu(z)\rangle\langle \phi_\nu(z)|\phi_i(z)\rangle . \tag{3}$$

Since the remotely doped PBW structure depicted in Fig. 1(a) has reflection symmetry about the center of the well, the envelope functions in Eq. (3) have definite parity, and it is clear that for the matrix element to be nonzero all three states must have the same parity. The envelope functions associated with the lowest subbands of the CB, VB, and SOB all have even parity, and alternate parity for higher subbands as indicated in Fig. 4. Thus, for example, the lowest-energy-allowed inelastic scattering intersubband transition is from the first to the third CB subband, CB(1)→CB(3), resonant off the lowest SOB subband, SOB(1), and the next lowest-energy transition from CB(1) is CB(1)→CB(5), as depicted in Fig. 4. For the assumed square-well-like potentials, the two splittings referred to above have the ratio $(3^2-1^2)/(5^2-1^2)=\frac{1}{3}$. The transition energies are independent of $\mathbf{k}$ assuming parabolic subbands and subband index independent effective masses, assumptions appropriate for the small $\mathbf{k}$'s and low-order subbands considered here. Thus, summing over the contributions from all $\mathbf{k}$ obeying the occupancy requirements for the various bands discussed earlier, the two scattering peaks resulting from the two transitions

depicted in Fig. 4 should have energy shifts with a ratio $\frac{1}{3}$.

We will now use this model to analyze our measurements on samples 1 and 2. For sample, 1, we assume an effective well width of $w_{\text{eff}} = \sim 1900 \pm 250$ Å, determined from the measured n_s, and an average electron effective mass of $m_e^* = 0.071 m_0$, determined by averaging the Al concentration dependent mass over the width of the slab. Then the square-well-like levels are calculated to have splittings of $E_{\text{CB}(3)} - E_{\text{CB}(1)} = 1.1 \pm 0.2$ meV and $E_{\text{CB}(5)} - E_{\text{CB}(1)} = 3.4 \pm 0.6$ meV, compared to the measured energy shifts of 0.85 ± 0.2 and 3.0 ± 0.3 meV, respectively. These measured energy shifts for the two peaks have the ratio $0.85/3.0 \approx 0.28 \pm 0.07$, consistent within the error bars with the $\frac{1}{3}$ ratio expected for square wells. Equations (1) and (2) predict that for vertical transitions using the same intermediate state, the peaks of the resonance curves for two different final-state subbands CB(f) and CB(f') should have an energy separation of $\Delta E \cong (E_{\text{CB}(f')} - E_{\text{CB}(f)})$. For sample 1 the scattering peaks are separated by 2.15 ± 0.4 meV, which is approximately equal to the separation of the resonance curve peaks, 2.0 ± 0.4 meV. The resonance curve widths of 2.5 and 3.0 meV are on the order of the calculated Fermi level $E_F = 2.9$ meV for this structure, as expected.

For sample 2, we assume an effective well width of $w_{\text{eff}} = \sim 2900 \pm 400$ Å, determined from the measured n_s, and an average electron effective mass of $m_e^* = 0.070 m_0$, determined by averaging the mass over the width of the slab. Then the square-well-like levels are calculated to have splittings of $E_{\text{CB}(3)} - E_{\text{CB}(1)} = 0.52 \pm 0.15$ meV and $E_{\text{CB}(5)} - E_{\text{CB}(1)} = 1.6 \pm 0.5$ meV, compared to the measured energy shifts of 0.65 ± 0.10 and 2.0 ± 0.2 meV, respectively. These measured energy shifts for the two peaks have the ratio $0.65/2.0 \approx 0.33 \pm 0.06$, approximately equal to the $\frac{1}{3}$ ratio expected for square wells. The peak spacing of 1.35 ± 0.2 meV is consistent with the separation between the resonance maximum excitation energies for the two peaks, 1.5 ± 0.5 meV.

Inelastic scattering involving other intersubband spin-flip transitions are allowed for this structure. For example, for the same lowest-energy SOB subband intermediate state, SOB(1), the transition CB(3)→CB(5) is allowed. Also, using SOB(2) (odd parity) as intermediate-state, transitions CB(2)→CB(4), CB(2)→CB(6), and CB(4) →CB(6) are allowed. None of these are evident in the spectra. There are several possible reasons for this. When SOB(2) is used as an intermediate state, by Eqs. (1) and (2), the resonance maxima should be shifted up in energy by an amount $E_{\text{SOB}(2)} - E_{\text{SOB}(1)}$, which is 3.5 meV for sample 1. This results in maximum resonance excitation energies in the range where the photoluminescence starts to dominate the spectra as seen in Fig. 2, and thus this photoluminescence may swamp the scattering peaks. Also, as observed by Pinczuk *et al.*[2], peaks associated with higher subband transitions are weaker and broader than those associated with the lower subband transitions. Thus, for example, the peak associated with the transition CB(2)→CB(4) might be expected to be small compared to the CB(1)→CB(3) and CB(1)→CB(5) peaks. Thus, it is not unreasonable that the spectra would be dominated by the CB(1)→CB(3) and CB(1)→CB(5) transitions, indicated in Fig. 4.

V. CONCLUSIONS

Our measurements of the $z(y',x')\bar{z}$ inelastic light-scattering spectra of n-type remotely doped wide parabolic $Al_xGa_{1-x}As$ quantum wells have revealed, for two samples, two peaks with energy shifts in the ratio $\sim \frac{1}{3}$. For each sample, a series of spectra, for excitations in a range near the $E_0 + \Delta_0$ gap of the bulk material at the center of the well, shows the peaks to be strongly resonant with resonance widths $\lesssim E_F \sim 3$ meV. The resonance curves show the resonance maxima have an energy separation approximately equal to the scattering peak separation. Interpreting the peaks in the $z(y',x')\bar{z}$ spectra as single-particle spin-flip vertical transitions between CB subbands,[2,3,12,16] we have found the observed energy shifts quantitatively consistent with a model for the electron gas in the remotely doped PBW being distributed as a uniform density electron slab, with an effective square-well-like potential, giving rise to square-well-like subbands. This confirms calculations of the energy-level structure for this system, complementing evidence for this behavior from transport measurements,[7,8] and suggests that this technique could, in principle, be used to give a measure of the electron slab width. The sharpness of the resonances and the small size of the peak shifts discerned also attest to the sensitivity of this technique for measuring precise subband levels in heterostructure systems.

ACKNOWLEDGMENTS

The authors would like to thank John Baskey for his assistance on transport measurements. The work at Harvard University was supported by the Harvard Materials Research Laboratory under Grants Nos. NSF-DMR-89-20490 and NSF-DMR-91-19386. The work at UCSB was supported by the Air Force Office of Scientific Research under Grant No. AFOSR-91-0214.

[1] G. Abstreiter and K. Ploog, Phys. Rev. Lett. **42**, 1308 (1979).

[2] A. Pinczuk, H. L. Störmer, R. Dingle, J. M. Worlock, W. Wiegmann, and A. C. Gossard, Solid State Commun. **32**, 1001 (1979).

[3] E. Burstein, A. Pinczuk, and S. Buchner, in *Physics of Semiconductors 1978*, edited by B. L. H. Wilson (The Institute of Physics, London, 1979), p. 1231.

[4] A. Pinczuk, G. Abstreiter, R. Trommer, and M. Cardona, Solid State Commun. **30**, 429 (1979).

[5] J. Menéndez, A. Pinczuk, A. C. Gossard, M. G. Lamont, and F. Cerdeira, Solid State Commun. **61**, 601 (1987).

[6] M. Sundaram, A. C. Gossard, J. H. English, and R. M. Westervelt, Superlatt. Microstruct. **4**, 683 (1988).

[7] T. Sajoto, J. Jo, M. Santos, and M. Shayegan, Appl. Phys. Lett.

55, 1430 (1989).
[8]E. G. Gwinn, P. F. Hopkins, A. J. Rimberg, R. M. Westervelt, M. Sundaram, and A. C. Gossard, Phys. Rev. B **41**, 10 700 (1990).
[9]P. F. Hopkins, A. J. Rimberg, E. G. Gwinn, R. M. Westervelt, M. Sundaram, and A. C. Gossard, Appl. Phys. Lett. **57**, 2823 (1990).
[10]R. C. Miller, A. C. Gossard, D. A. Kleinman, and O. Munteanu, Phys. Rev. B **29**, 3740 (1984).
[11]A. J. Rimberg and R. M. Westervelt, Phys. Rev. B **40**, 3970 (1989).
[12]See, for example, G. Abstreiter, M. Cardona, and A. Pinczuk, in *Light Scattering in Solids IV,* edited by M. Cardona and G. Güntherodt (Springer, Berlin, 1984).
[13]A. Pinczuk, S. Schmitt-Rink, G. Danan, J. P. Valladares, L. N. Pfeiffer, and K. W. West, Phys. Rev. Lett. **63**, 1633 (1989).
[14]P. A. Wolff, Phys. Rev. Lett. **16**, 225 (1966).
[15]D. C. Hamilton and A. L. McWhorter, in *Light Scattering Spectra of Solids,* edited by G. B. Wright (Springer, Berlin, 1969), p. 309.
[16]A. Pinczuk, J. M. Worlock, H. L. Störmer, R. Dingle, W. Wiegmann, and A. C. Gossard, Surf. Sci. **98**, 126 (1980).